

---

**From:** Glenn Mitchell  
**Sent:** Wednesday, 26 October 2016 4:58 p.m.  
**To:** Leeza.Becroft@beca.com  
**Cc:** Kristy Rusher  
**Subject:** RE: Local Government Official Information request - 563581

Leeza, thank you for your enquiry. The majority of hazard analysis we have for the city is from reports commissioned by the Otago Regional Council, in particular the 2007 NIWA report you mention.

As a couple of potentially high risk communities in Dunedin were absent from that report, we commissioned NIWA to undertake an additional tsunami analysis for Aramoana and Harrington Point which I attach.

The Otago Regional Council reports are available online at <http://www.orc.govt.nz/Information-and-Services/Natural-Hazards/hazards/Tsunami/> . In addition the Ministry of Civil Defence Emergency Management hold research information at <http://www.civildefence.govt.nz/cdem-sector/cdem-research-/mcdem-research-projects-and-resources/>

Note that the studies to date indicate minimal risk for the central city area, but smaller coastal communities are at some risk. If you require any further information, please do not hesitate to contact me directly. My DDI is 03 474 3114.

Regards

Glenn Mitchell  
Emergency Management Officer, Training and Readiness  
**Dunedin City Council**

Level C, 54 Moray Place; P.O. Box 5045, Moray Place, Dunedin 9058, New Zealand  
Telephone: 03 477 4000; Fax 03 477 7997  
Email: [glenn.mitchell@dcc.govt.nz](mailto:glenn.mitchell@dcc.govt.nz)

[www.dunedin.govt.nz](http://www.dunedin.govt.nz)  
[twitter.com/@DnEmergency](https://twitter.com/@DnEmergency)  
[facebook.com/DnEmergency](https://facebook.com/DnEmergency)

# Modelling tsunami inundation of Aramoana and Harrington Point, Dunedin

A 1:500 year 50th percentile scenario

*Prepared for Dunedin City Council*

*September 2015*

Prepared by:

Emily Lane  
Jade Arnold  
Shaun Williams  
Julian Sykes



For any information regarding this report please contact:

Emily Lane  
Hydrodynamics Scientist  
Hydrodynamics  
+64-3-343 7856  
Emily.Lane@niwa.co.nz

National Institute of Water & Atmospheric Research Ltd  
PO Box 8602  
Riccarton  
Christchurch 8011

Phone +64 3 348 8987

NIWA CLIENT REPORT No: CHC2015-101  
Report date: September 2015  
NIWA Project: DCC15502

Quality Assurance Statement		
	Reviewed by:	David Plew
	Formatting checked by:	America Holdene
	Approved for release by:	Charles Pearson

---

© All rights reserved. This publication may not be reproduced or copied in any form without the permission of the copyright owner(s). Such permission is only to be given in accordance with the terms of the client's contract with NIWA. This copyright extends to all forms of copying and any storage of material in any kind of information retrieval system.

Whilst NIWA has used all reasonable endeavours to ensure that the information contained in this document is accurate, NIWA does not give any express or implied warranty as to the completeness of the information contained herein, or that it will be suitable for any purpose(s) other than those specifically contemplated during the Project or agreed by NIWA and the Client.

20 October 2015 2.18 p.m.



## Contents

<b>Executive summary .....</b>	<b>5</b>
<b>1 Introduction .....</b>	<b>7</b>
<b>2 Modelling far-field tsunami inundation .....</b>	<b>9</b>
2.1 Source model and initial conditions .....	9
2.2 Inundation modelling.....	11
2.3 Model outputs .....	14
<b>3 Peru subduction zone model results .....</b>	<b>15</b>
3.1 Time series .....	15
3.2 Maximum tsunami height.....	16
3.3 Maximum inundation and speed.....	17
<b>4 Comparison with previous tsunami modelling in Dunedin.....</b>	<b>21</b>
<b>5 Conclusion .....</b>	<b>25</b>
<b>6 References.....</b>	<b>26</b>
<b>Appendix A           GIS layers .....</b>	<b>28</b>

## Figures

Figure 1-1:	Dunedin map showing areas where inundation was modelled (red boxes). The primary locations of interest in this study are Aramoana and Harrington Point, with Dunedin inner harbour, South Dunedin and Blueskin Bay included for comparison with previous modelling	8
Figure 2-1:	Earthquake and tsunami source region in Peru. Image created by collating the initial conditions and final maximum wave heights for the three scenarios. Left Hand Panel (a, c, e) = zoom in of initial conditions in Peru for each scenario; colour scale runs from -10 to 10 m depth. Right Hand Panel (b, d, f) = corresponding maximum wave height over the Pacific for each scenario. Scenario 1 (a and b) consists of a 22.4 m vertical slip; Scenario 2 (c and d) a 17.6 m slip; and Scenario 3 (e and f) a 35.1 m vertical slip.	10
Figure 2-2:	Full grid used for the tsunami modelling. Colour represents water depth.	12
Figure 2-3:	Close up of inundation grid in the Dunedin region. The grid is coloured by elevation between -5 metres and 5 metres to emphasise the coastal regions. In the open ocean it has a resolution around 4 km which is refined to around 500 m at the coast. In the areas of interest in this study it is further refined to 15-20 m and a similar land grid resolution is created and merged with the bathymetric grid to create a seamless inundation grid. Numbered areas correspond to time series locations shown in Figure 3-1	13



Figure 3-1:	Time series comparison for the three rupture scenarios. Locations correspond to numbered areas in Figure 2-3. The 11 hours since the start of the simulation have been added to the time series. Also the tide has been subtracted to emphasize the tsunami.	15
Figure 3-2:	Predicted maximum tsunami height (m) along the Dunedin coastline over all three scenarios. The tide has been subtracted in order to emphasize the tsunami height only.	16
Figure 3-3:	Maximum inundation depth for Aramoana and Harrington Point assuming the largest wave arrived at MHWS, where MHWS = 1m above DVD1958.	17
Figure 3-4:	Maximum flow speed for Aramoana and Harrington Point assuming the largest wave arrived at MHWS, where MHWS = 1m above DVD1958.	18
Figure 3-5:	Maximum inundation depth for Aramoana and Harrington Point assuming the largest wave arrived at MHWS + 0.3 = 1.3 m. This projection provides indicative future inundation if sea level were to rise 30 cm above DVD1958.	18
Figure 3-6:	Maximum flow speed for Aramoana and Harrington Point assuming the largest wave arrived at MHWS + 0.3 = 1.3 m. This projection provides indicative future flow speed if sea level were to rise 30 cm above DVD1958.	19
Figure 3-7:	Maximum inundation depth for Aramoana and Harrington Point assuming the largest wave arrived at MHWS + 0.5 = 1.5 m. This projection provides indicative future inundation if sea level were to rise 50 cm above DVD1958.	19
Figure 3-8:	Maximum flow speed for Aramoana and Harrington Point assuming the largest wave arrived at MHWS + 0.5 = 1.5 m. This projection provides indicative future flow speed if sea level were to rise 50 cm above DVD1958.	20
Figure 4-1:	Maximum inundation depth for a similar far-field 1:500 year tsunami arriving in Dunedin inner harbour at MHWS (from previous study by Lane et al., 2007).	21
Figure 4-2:	Maximum inundation depth from the present study for Dunedin inner harbour assuming the largest wave arrived at MHWS, where MHWS = 1m above DVD1958.	22
Figure 4-3:	Maximum water depth for a similar far-field 1:500 year tsunami arriving in South Dunedin at MHWS (from previous study by Lane et al., 2007).	23
Figure 4-4:	Maximum inundation depth from the present study for South Dunedin assuming the largest wave arrived at MHWS, where MHWS = 1m above DVD1958.	23
Figure 4-5:	Maximum water depth for a similar far-field 1:500 year tsunami arriving in Blueskin Bay at MHWS (from previous study by Lane et al., 2007).	24
Figure 4-6:	Maximum inundation depth from the present study for Blueskin Bay assuming the largest wave arrived at MHWS, where MHWS = 1m above DVD1958.	24



## Executive summary

- NIWA was commissioned by the Dunedin City Council (DCC) to undertake a numerical tsunami inundation modelling study of Aramoana and Harrington Point using a 1:500 year 50<sup>th</sup> percentile scenario from the 2013 Tsunami Hazard Review (Power 2013).
- The most likely scenario for a 1:500 year 50<sup>th</sup> percentile event is a magnitude 9.3 subduction zone earthquake source originating in Peru. This scenario is not considered a worst-case, but is useful for comparison with other coastal hazards.
- The source models (initial conditions) enabling this modelling were guided by the GNS tsunami database and the source segment used was taken from Tang et al. (2010). Three scenarios associated with this source were modelled and the results presented are the maximum of the three scenarios.
- The three scenarios chosen for this modelling have the same moment magnitude but with different configurations of segments rupturing and different skip amounts.
- Two numerical models were used to model the tsunami; Gerris and RiCOM. Gerris enabled trans-Pacific modelling from source to form the boundary conditions for higher resolution inundation modelling using RiCOM.
- The arrival of the largest modelled wave was assumed to coincide with Mean High Water Spring (MHWS) which was taken to be 1 m above the Dunedin Vertical Datum 1958 (DVD1958). Inundation was also modelled for two sea level rise scenarios (MHWS + 30 cm and MHWS + 50 cm) which is considered useful for long-term coastal hazard planning.
- The first modelled wave reached Aramoana and Harrington Point around 16 hours after fault rupture. The second and third waves, which are the largest, arrived between 17 – 19 hours after rupture.
- Aramoana exhibits greater inundation extent compared to Harrington Point with the majority of inundation up to 1.5 m, and exceeding 2.5 m in localised areas confined to the immediate coastline. Maximum tsunami height in the region of Dunedin is around 4.5 m above Dunedin Vertical Datum 1958 (DVD1958), which is slightly lower than the predicted 4.77 m in the 2013 Tsunami Hazard Review. This difference may be due to the approximation in the probabilistic tsunami modelling approach used in the 2013 Tsunami Hazard Review, and/or differences in the initial conditions used.
- Inundation extents, particularly at Aramoana, are increasingly greater for the two sea level rise scenarios MHWS + 30 cm and MHWS + 50 cm, respectively.
- Previous modelled results for the Dunedin inner harbour, South Dunedin and Blueskin Bay areas for a similar 1:500 year far-field event originating in South America, show lesser inundation extents compared to modelling results produced for these areas in this study. The variations reflect the simpler initial conditions used in the previous modelling. Inundation results presented in this report are considered more accurate for the 1:500 year tsunami in these areas.

- Tsunami flow speeds exceeding 2.5 m/s are observed at the harbour entrance, although these values should be treated as minimums due to the complexities in fully resolving small scale harbour currents at the resolution used in this modelling.

### Use of this report

The main purpose of this report is to help inform evacuation planning and emergency management planning. The scenario modelled has a high return period in the order of 500 years and represents a moderate to severe, but not worst-case, scenario that is appropriate for evacuation and emergency management planning. Information provided in this report may also be useful for land-use, strategic development, and infrastructure planning as it may, when used with other hazard information, highlight areas of higher vulnerability where future development should be more carefully managed. The spatial data in these layers have been generated at a scale of 1:25,000 and should not be used at scales finer than this.

### Caveat

This report is based on state-of-the-art knowledge and modelling capabilities of tsunamis and tsunami inundation. While every effort is made to provide accurate information, there are many uncertainties involved including knowledge of potential tsunami sources, source characteristics, bathymetry and topography. In addition, while the hydrodynamic models capture much of the physics involved in tsunami propagation and inundation, they also include some simplifying assumptions as with all models. The information provided in this report is of a technical nature and should be considered with the above limitations in mind.



## 1 Introduction

The Dunedin coast lies along the western edge of the Pacific Ocean and is exposed to local, regional, and distant-source tsunami risk. NIWA was contracted by the Dunedin City Council to undertake tsunami inundation modelling of Aramoana and Harrington Point using a 1:500 year 50<sup>th</sup> percentile scenario from the 2013 Tsunami Hazard Review (Power 2013). The most likely scenario for a 1:500 year 50<sup>th</sup> percentile event is a magnitude 9.3 subduction zone earthquake source originating in Peru. Inundation modelling for Dunedin Harbour, South Dunedin and Blueskin Bay using this scenario is also conducted for comparison with previous tsunami inundation modelling of the Otago coastline.

This report models a tsunami generated from the Peru earthquake source. The overarching scenario was guided by the GNS tsunami database and uses the source segment in Tang et al. (2010). Three earthquake rupture scenarios were chosen which all use the same moment magnitude but with different configurations of rupturing segments and displacements.

Inundation was modelled using three sea level scenarios consistent with previous modelling in the Dunedin area by Lane et al. (2007). These scenarios are:

- Mean High Water Spring tide (MHWS)
- MHWS + 30 cm
- MHWS + 50 cm

The latter two scenarios account for the likely future tsunami inundation hazard associated with projected sea level rise due to climate change.

Time series of offshore water levels are provided for each rupture scenario, as well as ascii raster files of maximum inundation depth and maximum flow speed for the following places (Figure 1-1):

- Aramoana
- Harrington Point

Figure 1-1 shows the regions where tsunami inundation was modelled. Note that maximum inundation depths at MHWS were also modelled for Dunedin Harbour, South Dunedin and Blueskin Bay for comparison with previous modelling in these areas. The baseline water level for the modelling is set at MHWS. This represents the case where the largest wave arrives in conjunction with high tide for an average spring tide. If there is a train of large waves, at least one wave will probably arrive close to high tide. If there is a single wave considerably larger than all the other tsunami waves, then the state of the tide when that wave arrives is important. These parameters are taken into account for each sea level scenario in this study at each site.

The results presented reflect the maximum of the three rupture scenarios and are discussed in terms of the inundation hazard at the investigated areas. Conclusions are provided for consideration in tsunami hazard, evacuation, and emergency management planning.



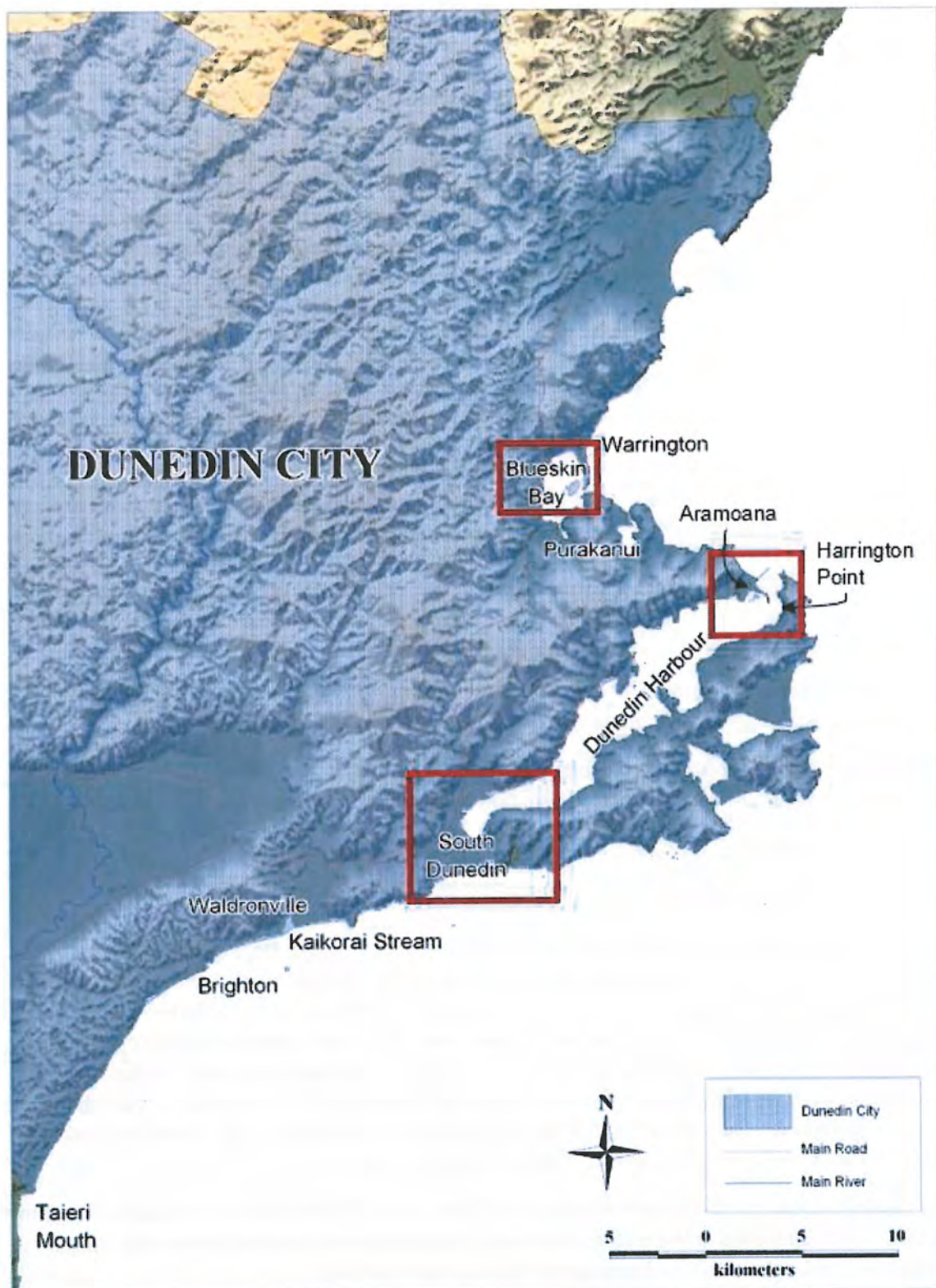


**Figure 1-1: Dunedin map showing areas where inundation was modelled (red boxes). The primary locations of interest in this study are Aramoana and Harrington Point, with Dunedin inner harbour, South Dunedin and Blueskin Bay included for comparison with previous modelling**



## 2 Modelling far-field tsunami inundation

### 2.1 Source model and initial conditions

The 2013 Tsunami Review (Power 2013) provides the wave height at the Dunedin coast for a 1:500 year tsunami as 4.77 m at the 50<sup>th</sup> percentile uncertainty level<sup>1</sup>. The most likely scenario for the 1:500 year event at the 50<sup>th</sup> percentile is a magnitude 9.3 earthquake originating in Peru. Therefore a magnitude 9.3 earthquake in Peru is used as the tsunami source in this study. The overarching scenario was guided by the GNS tsunami database and uses the source segment from Tang et al. (2010). Three earthquake rupture scenarios were selected which all use the same moment magnitude but with different configurations of rupturing segments and corresponding displacements (Figure 2-1). The first rupture scenario involves a 22.4 m slip, the second a 17.6 m slip, and the third a 35.1 m slip, with the overall maximum of the three scenarios reported in the results. In most cases however, this corresponds to the third scenario. The GNS tsunami database shows that a tsunami originating from this source region (77° W, 14° S) has more impact on the Otago peninsula than tsunamis originating north or south of there.

The tsunami is modelled from source across the Pacific Ocean using Gerris. The results are used as boundary conditions at the edge of the inundation grid (192.5° E) to model the tsunami inundation using RiCOM at the specified locations.

Fault movement is normally rapid when compared to time scales for wave propagation. Due to the incompressible nature of water, the instantaneous initial conditions on the water surface are the same as the ground surface displacement. This modelling strategy is adopted for the fault rupture scenarios presented here. Essentially the tsunami starts with zero velocity and a water surface displacement given by the estimates for seabed displacement. The wave then evolves in time as a long gravity wave.

In terms of sea level, the difference between the maximum wave arriving in conjunction with high tide or with low tide can be up to 2.11 m in Dunedin Harbour, which includes Aramoana, Harrington Point and South Dunedin (LINZ tidal levels at NZ ports: <http://www.linz.govt.nz/data/geodetic-system/datums-projections-heights/vertical-datums/tidal-level-information-surveyors>). This represents the mean tidal range if non-linear interaction occurred. Based on this, MHWS for Aramoana is taken as 1 m above Dunedin Vertical Datum 1958 (DVD1958). Thus, the three sea level scenarios used in this investigation are modelled with fixed elevations of:

- MHWS = 1 m
- MHWS + 30cm = 1.3 m
- MHWS + 50 cm = 1.5 m

with the latter two scenarios taking into account sea level rise due to climate change.

---

<sup>1</sup> In probabilistic tsunami hazard assessment, the 50<sup>th</sup> percentile uncertainty level refers to the relative contribution of different fault sources to the median hazard at 500 years (see Power 2013 for further details).



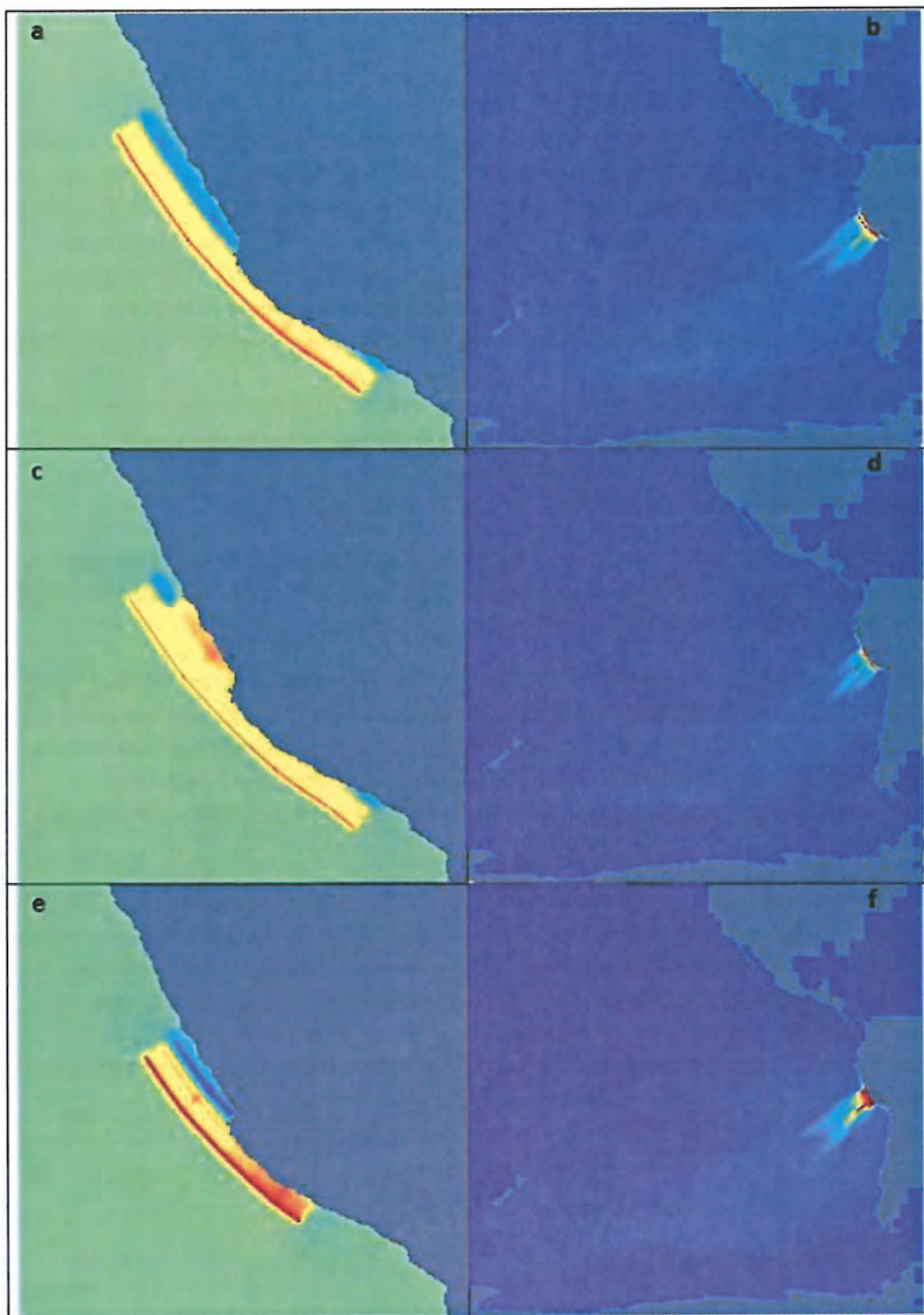


**Figure 2-1: Earthquake and tsunami source region in Peru. Image created by collating the initial conditions and final maximum wave heights for the three scenarios. Left Hand Panel (a, c, e) = zoom in of initial conditions in Peru for each scenario; colour scale runs from -10 to 10 m depth. Right Hand Panel (b, d, f) = corresponding maximum wave height over the Pacific for each scenario. Scenario 1 (a and b) consists of a 22.4 m vertical slip; Scenario 2 (c and d) a 17.6 m slip; and Scenario 3 (e and f) a 35.1 m vertical slip.**



## 2.2 Inundation modelling

### 2.2.1 Inundation models

Two models were used for the inundation modelling in this report. Gerris was used to model the trans-Pacific tsunami propagation from source, forming the boundary conditions for the higher resolution inundation modelling carried out using RiCOM.

Gerris is an open source partial differential equation solver based on adaptive Cartesian meshes using a quadtree format. This enables the mesh to adaptively refine or coarsen to resolve the tsunami wave crests within a specific error.

RiCOM has been developed over the last few decades and has been used for tsunami inundation modelling for a range of scenarios in NZ (Walters and Casulli 1998a; Walters 2005a; Walters 2005b; Walters et al. 2006a; Walters et al. 2006b; Lane et al. 2007; Walters et al. 2007; Walters et al. 2009; Gillibrand et al. 2010; Gillibrand et al. 2011; Lane et al. 2011).

RiCOM is based on the Reynolds-averaged Navier-Stokes (RANS) equations and the incompressibility criterion. For this modelling the hydrostatic assumption (that the vertical pressure gradient is balanced by gravity) is also made which reduces the equations to the non-linear shallow water equations (NLSWE). Research has shown that these equations adequately model tsunami inundation in the case of non-breaking waves (Pederson 2008). The time steps the model solves for are handled by a semi-implicit numerical scheme that avoids stability constraints on wave propagation. The advection scheme is semi-Lagrangian, which is robust, stable, and efficient (Staniforth and Côté 1991). Wetting and drying of intertidal or flooded areas occurs naturally with this formulation and is a consequence of the finite volume form of the continuity equation and method of calculating fluxes (flows) through the triangular element faces. Friction is enhanced for shallow water to account for the turbulent nature of tsunami flows but a spatially varying bed roughness is not used. At open (sea) boundaries, a radiation condition is enforced so that outgoing waves will not reflect back into the study area, but instead are allowed to realistically continue “through” this artificial boundary and into the open sea. The equations are solved with a conjugate-gradient iterative solver. The details of the numerical approximations that lead to the required robustness and efficiency may be found in Walters and Casulli (1998b) and Walters (2005b).

Both models were run with an initially quiescent sea state set at a level chosen to represent the tidal height at the arrival of the maximum wave (in this case MHWS). In the open ocean tidal amplitudes are small relative to water depth with low velocities that are unlikely to affect tsunami wave speed. Thus, trans-Pacific modelling using Gerris was carried out at zero sea level which was adequate to form the boundary conditions to model the tsunami arriving during MHWS using RiCOM.

### 2.2.2 Model grid – bathymetry and topography

The simulation of inundation is strongly dependent on the quality of the topographic data and the bathymetric data in inshore waters. For this modelling, LiDAR data obtained from DCC for the land topography and data obtained from Port Otago for the near-shore bathymetry in the vicinity of Aramoana and Harrington point were used.

A bathymetric grid covering New Zealand’s Exclusive Economic Zone (EEZ) was used as a base grid. This was cut down to cover from the east coast of New Zealand (East Cape to Dunedin) to 192.5° E. In the open ocean the grid has a resolution around 4 km which is refined to around 500 m at the coast. In the areas of interest in this study it is further refined to 15-20 m and a land grid at a similar



resolution is created and attached to the bathymetric grid to create a seamless inundation grid. Open ocean bathymetry at 30 second resolution (GEBCO 2013) was incorporated with bathymetry provided by Port Otago, along with NIWA in-house bathymetry for coastal New Zealand.

The land grid covers the areas of interest expected to be inundated. Inundation grids have been developed with specific high resolution where it is needed for inundation including resolved harbour Islands. Figure 2-2 shows an example of the full grid used for the tsunami modelling and Figure 2-3 shows a close-up of the land grid for inundation modelling. Land areas for Dunedin City and South Dunedin were also included for comparison with previous tsunami modelling (Lane et al. 2007). LiDAR data provided by Dunedin City Council was used to create the land topography. The vertical datum used in the grid is Dunedin Vertical Datum 1958.

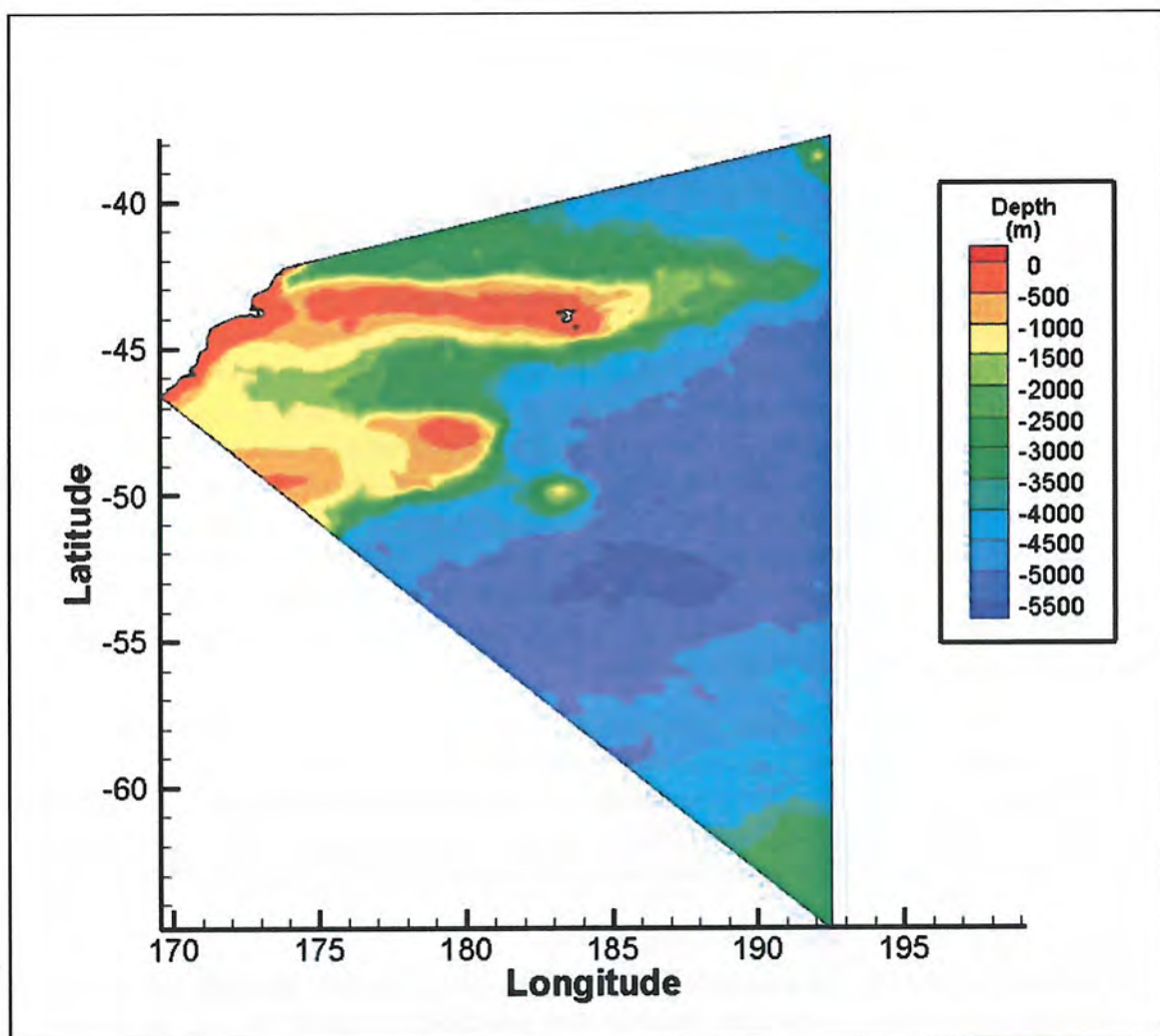


**Figure 2-2:** Full grid used for the tsunami modelling. Colour represents water depth.

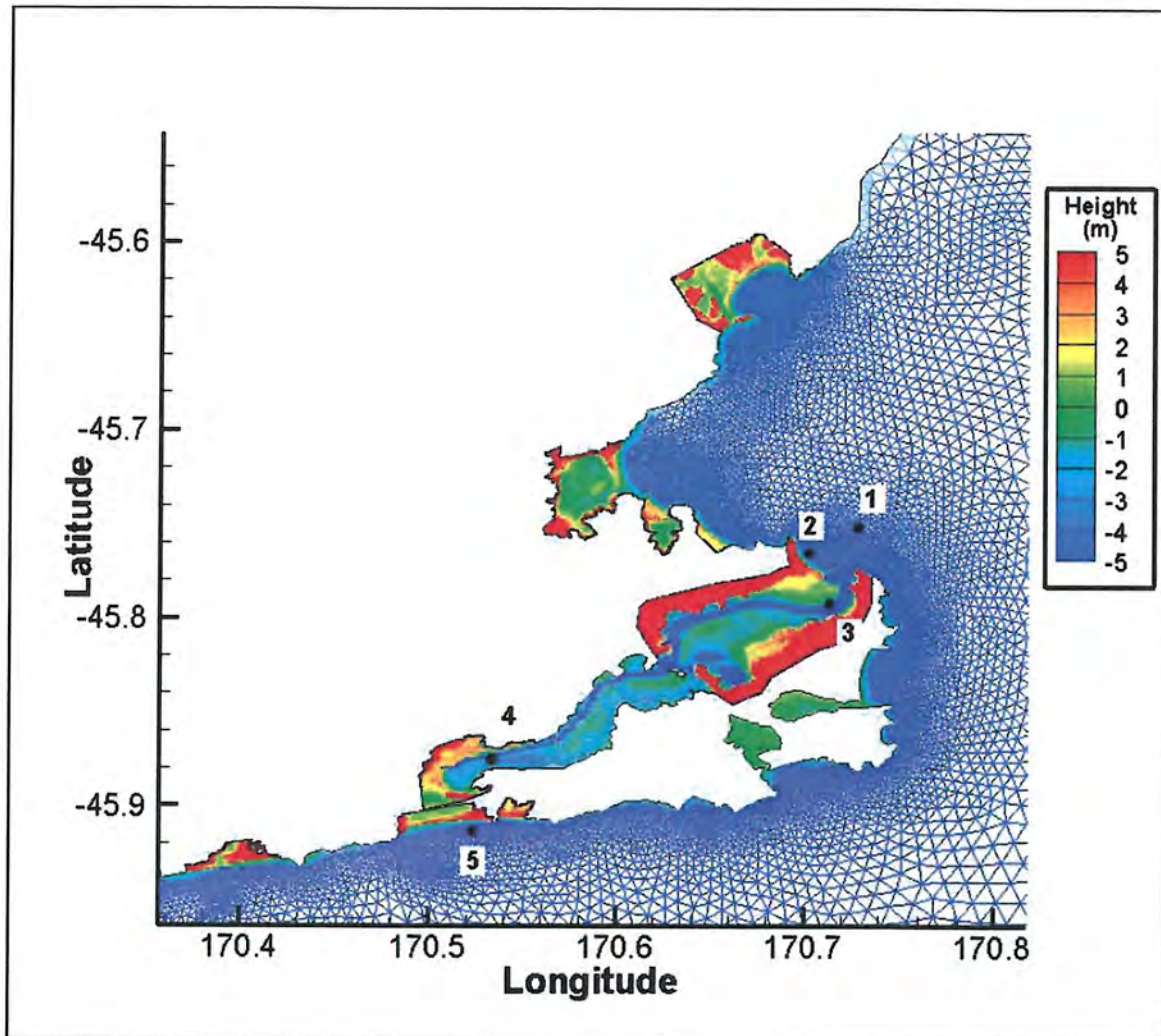


Figure 2-3: Close up of inundation grid in the Dunedin region. The grid is coloured by elevation between -5 metres and 5 metres to emphasise the coastal regions. In the open ocean it has a resolution around 4 km which is refined to around 500 m at the coast. In the areas of interest in this study it is further refined to 15-20 m and a similar land grid resolution is created and merged with the bathymetric grid to create a seamless inundation grid. Numbered areas correspond to time series locations shown in Figure 3-1

### 2.2.3 Uncertainties

The simulation of inundation is strongly dependent on the quality of the topographic data and the bathymetric data in inshore waters. For this modelling we have LiDAR data for the land topography and high resolution near-shore bathymetry in the vicinity of Dunedin, but in order to capture some of the more complex small scale processes in harbours, higher resolution data is required.

Other uncertainties in the modelling study include the gridded representation of a continuous coastline, which can deform the shape of bays and estuaries, and the effects of building and land features on form drag. The latter could substantially modify the onshore propagation of tsunamis. Improving the drag representation remains a goal of current research. Eradication of the other errors is constrained by limitations of data quality and the practicalities of grid resolution; models always represent an approximation of reality.



Model uncertainty can be quantified by running multiple simulations with small variations in key parameters, an approach known as ensemble prediction or sensitivity analysis. Such an approach provides an envelope of predicted solutions, rather than single “worst-case” or “scenario-type” predictions, on which to base emergency response procedures. However, running many simulations increases the computational and research costs, and, in any event, model forecasts can never be certain because our knowledge of all the geophysical processes involved in tsunami generation, propagation and inundation remains incomplete. In this report we run three scenarios with the same moment magnitude to cover a range of possible fault geometries, with results representing the maximum of the three scenarios.

Quantitative calibration of the tsunami inundation model against real measurements is difficult due to the uncertain nature of tsunami impact data from New Zealand and the consequent difficulty in identifying events from the past. Nevertheless, both the RiCOM model and the Gerris model have been continuously validated against standard analytical test cases (e.g. Walters and Casulli 1998b; Walters 2005b; Walters 2005a; Popinet 2003; Popinet 2011; Popinet 2012), thus providing credible results.

## 2.3 Model outputs

The outputs listed below were produced using the numerical models:

- A. Maps of maximum wave heights (relative to mean sea level).
- B. Spatial data depicting the depth and extent of coastal inundation at the specified areas for the largest wave arriving at MHWS, MHWS + 30 cm, and MHWS + 50 cm. The inundation depth is the depth of water on land (i.e. it is not referenced to mean sea level). If this data is used with a topographic representation different from that used in the model, then spurious results may occur.
- C. Spatial data depicting the maximum flow speed over land in the specified areas for the largest wave arriving at MHWS, MHWS + 30 cm, and MHWS + 50 cm.

These outputs describe the propagation and magnitude of the tsunami arriving at the Dunedin coastline, and the inundation at the specified locations.

The spatial maps are presented and discussed in this report. The spatial data (in ArcGIS format) is provided to Dunedin City Council along with this report in the CD enclosed as Appendix A.

### 3 Peru subduction zone model results

In the Dunedin region, the first wave for all three scenarios arrives within 16 hours of fault rupture with the second and third (and generally largest) waves arriving 17 – 19 hours after rupture (Figure 3-1). Some variation between the three scenarios can be observed but all three generally showed similar patterns. Resonance amplification starts to diminish after the fourth wave (particularly for Scenario 3), with weak amplification lingering for at least 10 hours after the first wave arrival.

#### 3.1 Time series

Figure 3-1 shows the time series for the three rupture scenarios at the numbered locations in Figure 2-3. Scenario 3, having the largest vertical slip at rupture, generally produces the worst-case tsunami results for all of the time series (TS) locations (with the exception of TS-4). Virtually no significant tsunami waves are observed at TS-4, suggesting negligible impacts in this area from a tsunami generated if the rupture scenarios presented in this report were to occur. However, it is worth noting that TS-4 is located in the inner harbour (Figure 2-3) and the reason for the very little response is because the area is protected by the narrow harbour opening as well as the inner harbour islands. Figure 3-2 shows how much of the tsunami reaches into the harbour, which generally makes it into the outer portion but not significantly into the inner part.

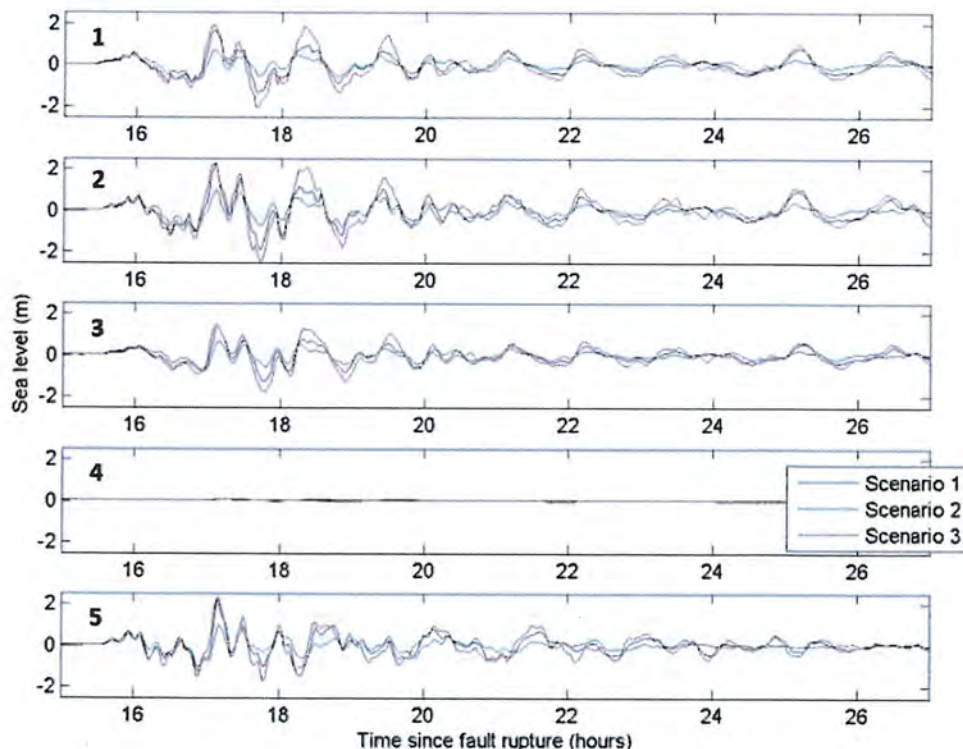


**Figure 3-1: Time series comparison for the three rupture scenarios. Locations correspond to numbered areas in Figure 2-3. The 11 hours since the start of the simulation have been added to the time series. Also the tide has been subtracted to emphasize the tsunami.**



### 3.2 Maximum tsunami height

The maximum predicted tsunami height for the Dunedin coast is shown in Figure 3-2. The values shown are provided relative to the undisturbed water level and do not include the MHWS offset that the inundation modelling includes. The actual water level can be obtained by adding the tidal water level at the time of the wave arrival. Maximum tsunami height in the region of Dunedin is around 4.5 m, which is slightly lower than the predicted 4.77 m in the 2013 Tsunami Hazard Review. This variation may be due to the approximation in the probabilistic tsunami modelling used in the 2013 Tsunami Hazard Review, and/or differences in the initial conditions used.

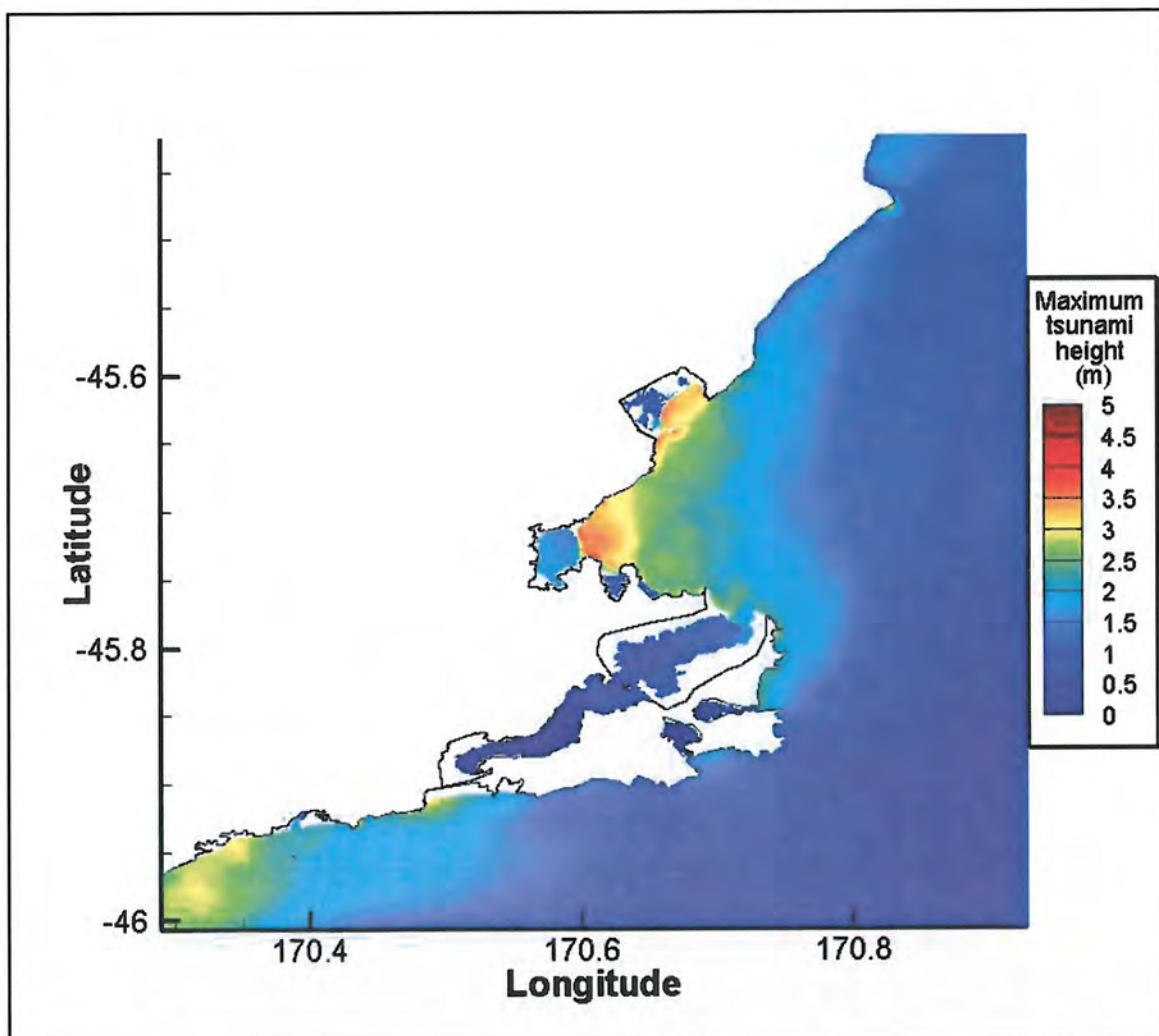


**Figure 3-2: Predicted maximum tsunami height (m) along the Dunedin coastline over all three scenarios. The tide has been subtracted in order to emphasize the tsunami height only.**

### 3.3 Maximum inundation and speed

Maximum inundation depth and maximum flow speed are presented for Aramoana and Harrington Point. Maximum inundation is the inundation that would occur if the arrival of the largest wave at a particular location (not necessarily the first wave and not necessarily the same wave in different areas) coincided with MHWS. It should be noted that the maximum inundation and speed maps presented are for illustration purposes only and reflect the conglomerate maximum of the three rupture scenarios used. The full GIS digital spatial data files are included on CD as Appendix A. For this simulation the second and third waves are the largest, particularly for TS locations 1, 2 and 3.

For the cases of Aramoana and Harrington Point, figures showing maximum inundation depth and maximum flow speed are given for three sea level scenarios. Figure 3-3 and Figure 3-4 show maximum inundation depth and speed, respectively, if the tsunami was to arrive at present-day MHWS. Figure 3-5 and Figure 3-6 show maximum inundation depth and speed accounting for sea level rise projections if the tsunami was to arrive at MHWS + 30 cm, while Figure 3-7 and Figure 3-8 depict maximum inundation depth and speed if the tsunami was to arrive at MHWS + 50 cm. Inundation depths are provided over the land only, whereas speeds are given for the sea as well as inundated areas of the land. The accompanying GIS files in Appendix A should be consulted for further details.

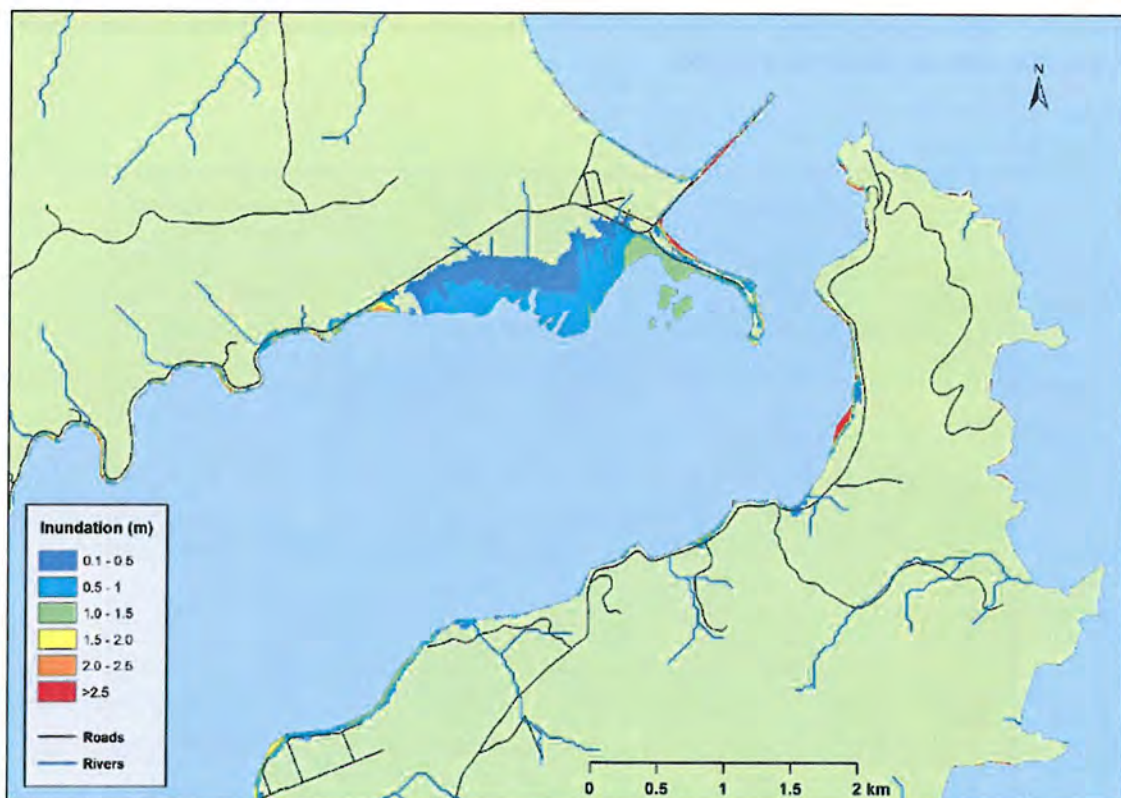


**Figure 3-3: Maximum inundation depth for Aramoana and Harrington Point assuming the largest wave arrived at MHWS, where MHWS = 1m above DVD1958.**



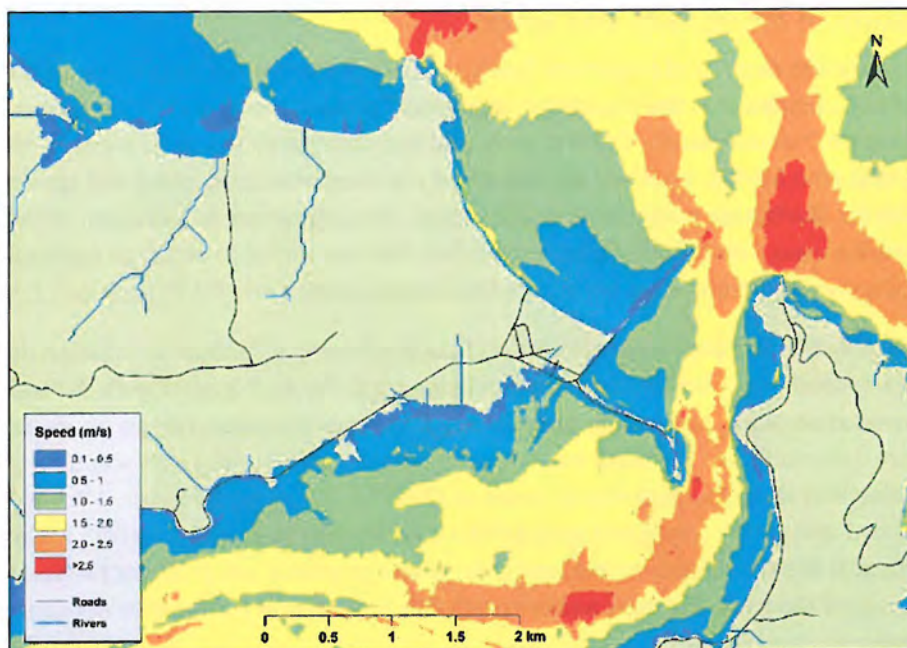


**Figure 3-4: Maximum flow speed for Aramoana and Harrington Point assuming the largest wave arrived at MHWS, where MHWS = 1m above DVD1958.**

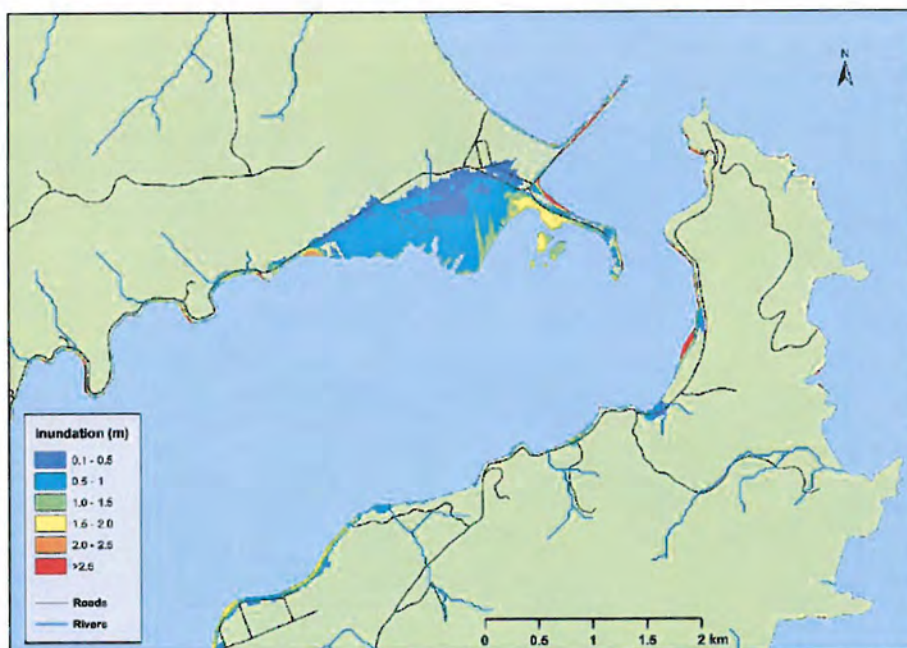


**Figure 3-5: Maximum inundation depth for Aramoana and Harrington Point assuming the largest wave arrived at MHWS + 0.3 = 1.3 m. This projection provides indicative future inundation if sea level were to rise 30 cm above DVD1958.**

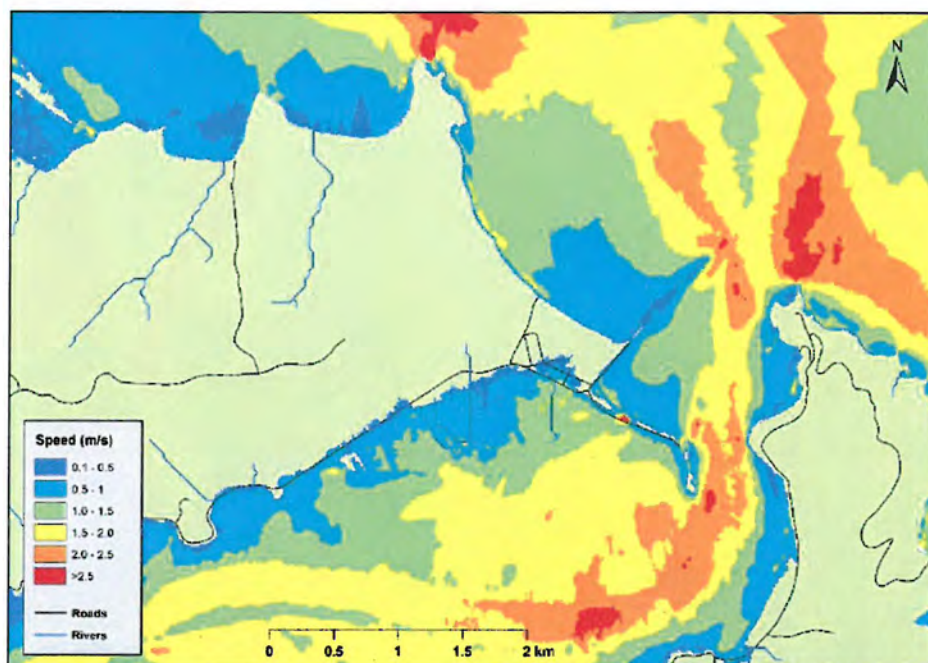


**Figure 3-6: Maximum flow speed for Aramoana and Harrington Point assuming the largest wave arrived at  $\text{MHWS} + 0.3 = 1.3 \text{ m}$ . This projection provides indicative future flow speed if sea level were to rise 30 cm above DVD1958.**

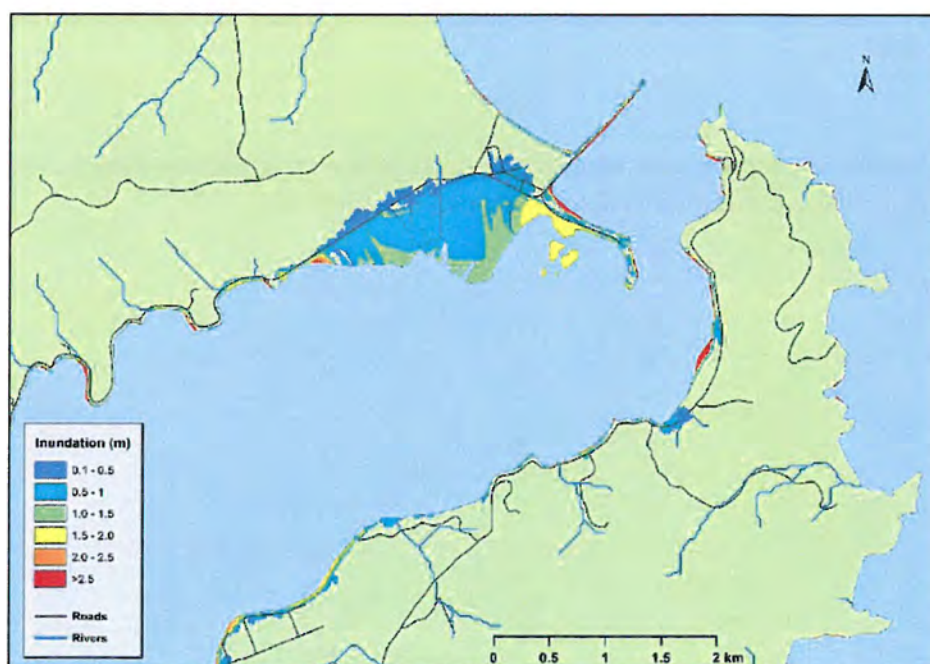


**Figure 3-7: Maximum inundation depth for Aramoana and Harrington Point assuming the largest wave arrived at  $\text{MHWS} + 0.5 = 1.5 \text{ m}$ . This projection provides indicative future inundation if sea level were to rise 50 cm above DVD1958.**



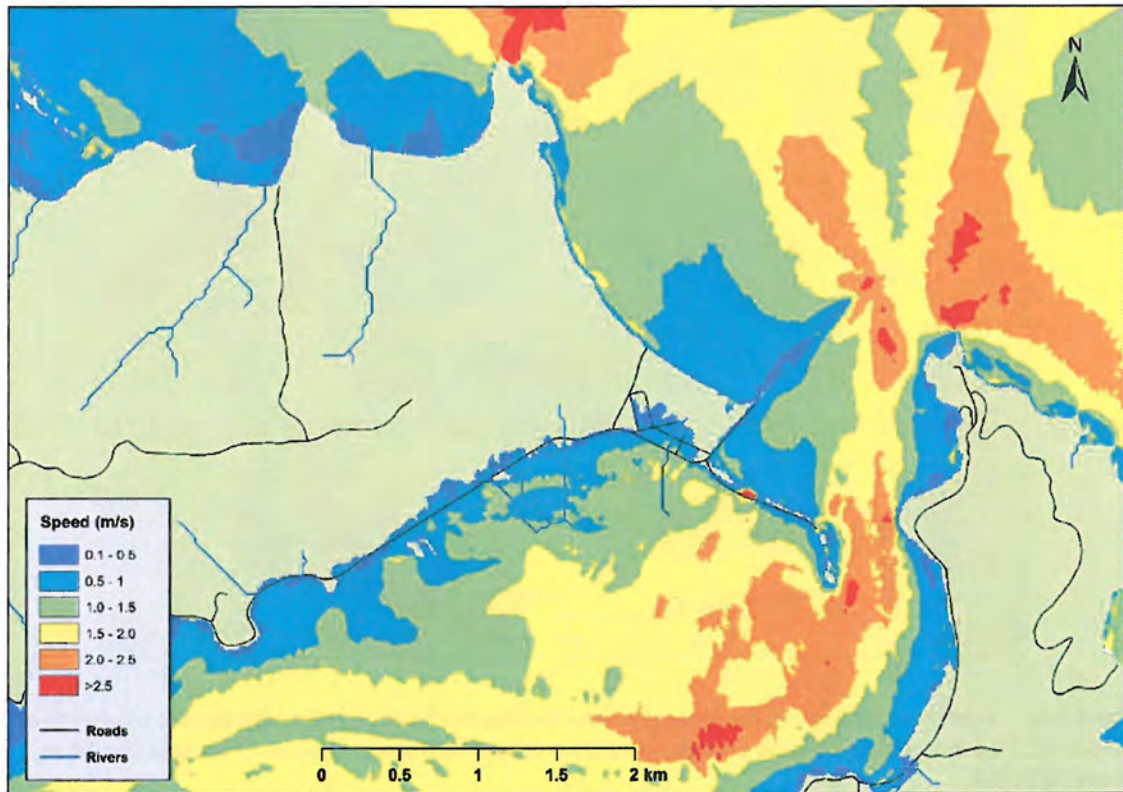


**Figure 3-8: Maximum flow speed for Aramoana and Harrington Point assuming the largest wave arrived at MHWS + 0.5 = 1.5 m. This projection provides indicative future flow speed if sea level were to rise 50 cm above DVD1958.**

These results generally show greater inundation extents at Aramoana and Harrington under sea level rise projections; which is useful for long-term planning consideration.

## 4 Comparison with previous tsunami modelling in Dunedin

Previous far-field tsunami modelling in the Otago area was conducted by Lane et al. (2007), with a similar 1:500 year South American source to the scenarios presented in this report. Maximum inundation depths at MHWS for the two modelling studies are compared for Dunedin inner harbour, South Dunedin and Blueskin Bay locations.

### 4.1.1 Dunedin inner harbour

Previous modelling suggested that there was not expected to be any significant tsunami inundation in the Dunedin inner harbour above what occurs regularly as normal water level fluctuations due to tidal and atmospheric forcing (Figure 4-1) (Lane et al., 2007).

Modelling presented here corroborates this observation (Figure 3-1 – TS-4, and Figure 4-2), with negligible inundation occurring around the inner harbour coastline.

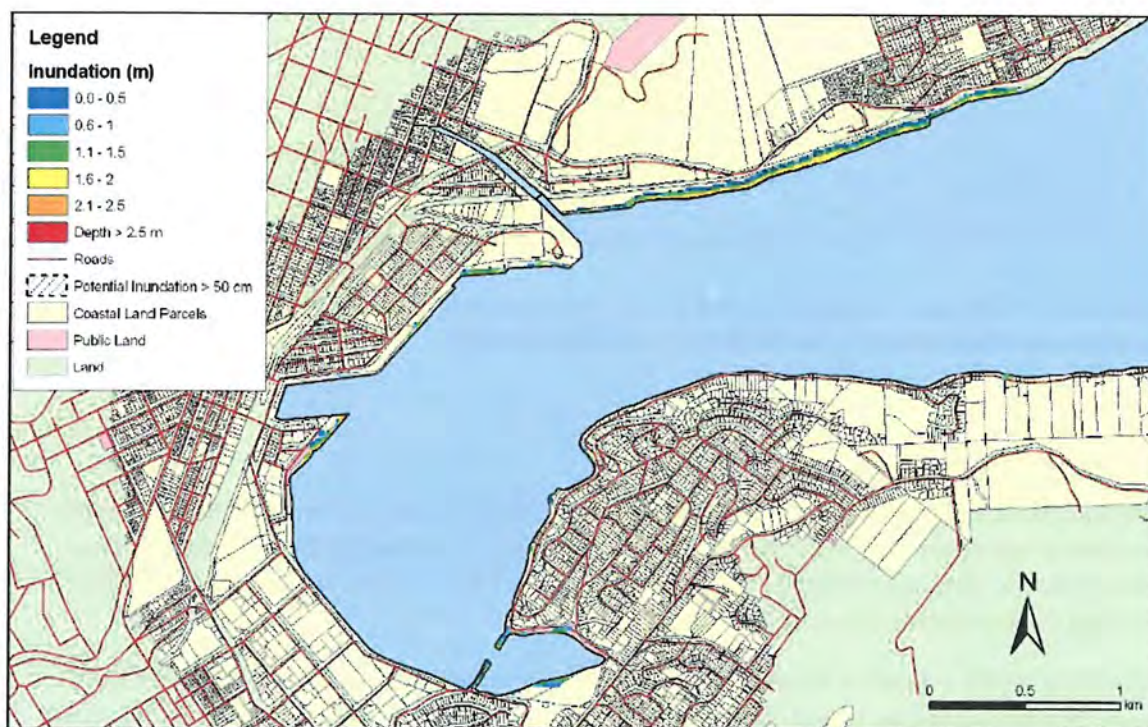


**Figure 4-1: Maximum inundation depth for a similar far-field 1:500 year tsunami arriving in Dunedin inner harbour at MHWS (from previous study by Lane et al., 2007).**



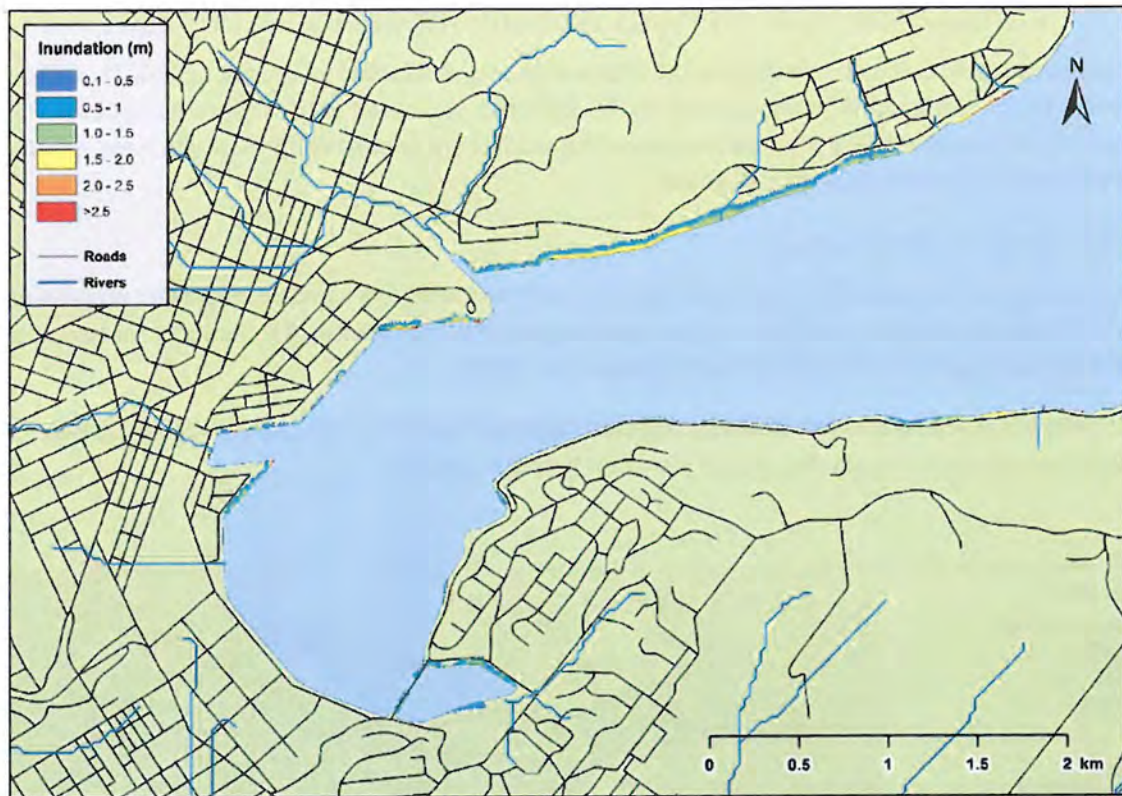


**Figure 4-2: Maximum inundation depth from the present study for Dunedin inner harbour assuming the largest wave arrived at MHWS, where MHWS = 1m above DVD1958.**

#### 4.1.2 South Dunedin

Previous work indicated that the third wave arriving at South Dunedin would be the highest with a maximum inundation depth of 2.3m for a 1:500 year tsunami (Lane et al. 2007). Inundation was determined to be confined to the coast with relatively low flow speeds, hence the risk of tsunami erosion was considered to be minimal (Figure 4-3).

Modelling results presented here indicate slightly greater inundation depths (> 2.5 m) but over a larger spatial extent (Figure 4-4). This variation can be explained by slight differences in the initial conditions (source models) used for the two studies, in which previous modelling was carried out using simpler initial conditions thereby influencing the subsequent tsunami characteristics.

Nevertheless, inundation results in this report corroborate previous observations in that inundation is confined to the immediate coastline, with relatively low risk of damaging impacts.





**Figure 4-3: Maximum water depth for a similar far-field 1:500 year tsunami arriving in South Dunedin at MHWS (from previous study by Lane et al., 2007).**



**Figure 4-4: Maximum inundation depth from the present study for South Dunedin assuming the largest wave arrived at MHWS, where MHWS = 1m above DVD1958.**



#### 4.1.3 Blueskin Bay

Consistent with this study, previous modelling suggested that the third wave arriving in Blueskin Bay would be the largest with a maximum run-up of 2.3 m for a 1:500 year tsunami (Figure 4-5) (Lane et al. 2007). The sand spit was overtopped in all previously modelled scenarios, which is consistent with modelling results in this report (Figure 4-6) where the sand spit is overtopped by inundation depths exceeding 2.5 m. Inundation appears more extensive in the new modelling results (Figure 4-6), but similar to the results for South Dunedin, these are explained by the more complex initial conditions used to generate the tsunami in this report.



**Figure 4-5:** Maximum water depth for a similar far-field 1:500 year tsunami arriving in Blueskin Bay at MHWS (from previous study by Lane et al., 2007).



**Figure 4-6:** Maximum inundation depth from the present study for Blueskin Bay assuming the largest wave arrived at MHWS, where MHWS = 1m above DVD1958.



## 5 Conclusion

This report models a tsunami generated from a far-field Peruvian fault source to assess the 1:500 year tsunami hazard at Aramoana and Harrington Point in Dunedin. The rupture scenarios used were guided by the GNS tsunami database with the source segments taken from Tang et al. (2010). Two numerical models, Gerris and RiCOM, are used to carry out the modelling in this study. Gerris was used to model the trans-Pacific tsunami propagation from source which formed the boundary conditions for the inundation modelling using RiCOM. Three rupture scenarios were used with the overall maximum inundation depths and flow speeds reported for three different sea level scenarios; MHWs, MHWs + 30 cm and MHWs + 50 cm. The latter two account for sea level rise if the tsunami were to occur in future.

Time series results indicate that the first wave arrives about 16 hours after fault rupture, with the second and third waves (largest waves) arriving within 17 – 19 hours after rupture. Maximum wave heights in the Dunedin region is around 4.5 m, although these are largely confined to the immediate coastline. Aramoana exhibits more extensive inundation than Harrington point, with the majority of inundated areas experiencing up to 1 m inundation depth.

The majority of flow speeds are between 0 – 2.5 m/s, with some exceeding 2.5 m/s around the harbour entrance. It should be noted that the modelling resolution here is around 15-20 m, which may not fully resolve the complex small scale currents that may occur in embayed or harboured areas. Thus the values provided should be treated as minimums.

The extent of inundation and maximum wave heights increases for higher sea level scenarios (MHWs + 30 cm and MHWs + 50 cm), particularly at Aramoana. This may be important for future planning which considers the impacts of sea level rise.

Inundation modelled at Dunedin inner harbour, South Dunedin and Blueskin Bay show slightly greater inundation extents than previously modelled results for these areas. The differences can be explained by the variations in the initial conditions used in both studies to model the 1:500 year tsunami. This report uses more complex initial conditions thereby providing more realistic tsunami characteristics. Hence the results presented in this study for these areas are considered more accurate than previous results.

The modelling presented in this report assumes a fixed bathymetry and topography. Large tsunamis waves could considerably erode dunes and other structures that they overtop which could leave the land behind them open to attack by subsequent waves. Rivers are not explicitly modelled with water in these simulations. The water in rivers could cause tsunami surges to travel further upstream than shown in these simulations, although it would not be expected to cause significant extra inundation.

Despite the inherent uncertainties in numerical modelling of tsunami inundation, we believe that the results presented in this report provides the best estimate of distant-source tsunami inundation of Dunedin available to date.



## 6 References

- GEBCO (2013) General Bathymetric Chart of the Oceans (GEBCO). <http://www.gebco.net/>
- Gillibrand, P.A., Arnold, J., Lane, E.M., Roulston, H., Enright, M. (2011) Modelling Coastal Inundation in Canterbury from a South American Tsunami. NIWA Client Report, CHC2011-009: 55 p.
- Gillibrand, P.A., Power, W.L., Lane, E.M., Wang, X., Sykes, J.R.E., Brackley, H., Arnold, J. (2010) Probabilistic hazard analysis and modelling of Tsunami inundation for the Auckland region from regional source Tsunami. NIWA Client Report: 62 p. : ill., maps, tables, refs p. 54-56. Q:\Library\Originals\Client Reps\2010
- Lane, E.M., Gillibrand, P.A., Arnold, J.R., Walters, R.A. (2011) Tsunami inundation modelling using RiCOM. Australian Journal of Civil Engineering, 9(1): 83-98
- Lane, E.M., Walters, R.A., Wild, M., Arnold, J., Enright, M., Roulston, H., Mountjoy, J. (2007) Otago region hazards management investigation: tsunami modelling study. NIWA Client Report, CHC2007-030: 253.
- Pederson, G. (2008) Modeling runup with depth integrated equation models. In: P.L.-F. Liu, H. Yeh & C. Synolakis (Eds). Advances in coastal and ocean engineering: Advanced numerical models for simulating tsunami waves and runup. World Scientific: 3-41.
- Popinet, S. (2003) Gerris: a tree-based adaptive solver for the incompressible Euler equations in complex geometries. Journal of Computational Physics, 190(2): 572-600. 10.1016/s0021-9991(03)00298-5
- Popinet, S. (2011) Quadtree-adaptive tsunami modelling. Ocean Dynamics, Vol. 61, no. 9.: 1261-1285. <http://dx.doi.org/10.1007/s10236-011-0438-z>
- Popinet, S. (2012) Adaptive modelling of long-distance wave propagation and fine-scale flooding during the Tohoku tsunami. Natural Hazards and Earth System Sciences, 12(4): 1213-1227. 10.5194/nhess-12-1213-2012
- Power, W.L. (2013) Review of Tsunami Hazard in New Zealand (2013 Update), GNS Science Consultancy Report 2013/131.
- Staniforth, A., Côté, J. (1991) Semi-Lagrangian integration schemes for atmospheric models - a review. Monthly Weather Review, 119(9): 2206-2223.
- Tang, L., Titov, V.V., Chamberlin, C.D. (2010) PMEL Tsunami Forecast Series: Vol. 1, A Tsunami forecast Model for Hilo, Hawaii. NOAA OAR Special Report, March 2010. 108 p.
- Walters, R.A. (2005a) Coastal ocean models: two useful finite element methods. Continental Shelf Research, 25(7-8): 775-793. 10.1016/j.csr.2004.09.020
- Walters, R.A. (2005b) A semi-implicit finite element model for non-hydrostatic (dispersive) surface waves. International Journal for Numerical Methods in Fluids, 49(7): 721-737. 10.1002/fld.1019

- Walters, R.A., Barnes, P., Goff, J.R. (2006a) Locally generated tsunami along the Kaikoura coastal margin: Part 1. Fault ruptures. *New Zealand Journal of Marine and Freshwater Research*, 40(1): 1-16. <Go to ISI>://WOS:000237691000001
- Walters, R.A., Barnes, P., Lewis, K., Goff, J.R. (2006b) Locally generated tsunami along the Kaikoura coastal margin: Part 2. Submarine landslides. *New Zealand Journal of Marine and Freshwater Research*, 40(1): 17-28. <Go to ISI>://WOS:000237691000002
- Walters, R.A., Casulli, V. (1998a) A robust, finite element model for hydrostatic surface water flows. *Communications in Numerical Methods in Engineering*, 14(10): 931-940. 10.1002/(sici)1099-0887(1998100)14:10<931::aid-cnm199>3.0.co;2-x
- Walters, R.A., Casulli, V. (1998b) A robust, finite element model for hydrostatic surface water flows. *Communications in Numerical Methods in Engineering*, 14: 931-940.
- Walters, R.A., Lane, E.M., Hanert, E. (2009) Useful time-stepping methods for the Coriolis term in a shallow water model. *Ocean Modelling*, 28(1-3): 66-74. 10.1016/j.ocemod.2008.10.004
- Walters, R.A., Lane, E.M., Henry, R.F. (2007) Semi-Lagrangian methods for a finite element coastal ocean model. *Ocean Modelling*, 19(3-4): 112-124. 10.1016/j.ocemod.2007.06.008



## Appendix A    GIS layers

The GIS rasters for Figure 3-2 through to Figure 3-8 are included in the CD in the case at the back of this report. The spatial data in these layers have been generated at a scale of 1:25,000 and should not be used at scales finer than this.